Scale and Transport Considerations on Piloted Ignition of PMMA

Richard T. Long Jr.[+], Jose L. Torero[*] and James G. Quintiere
Department of Fire Protection Engineering
University of Maryland
College Park, MD 20742-3031, USA

and

A.C. Fernandez-Pello
Department of Mechanical Engineering
University of California
Berkeley, CA 94720, USA

ABSTRACT

Experiments were performed to determine the effect of scale reduction and transport mechanisms on piloted ignition. Piloted ignition is commonly used as a reference for material flammability. The experimental methodology is that of the Lateral Ignition and Flame Spread Test (LIFT) and the fuel evaluated is commercial grade PMMA. It was observed that buoyancy effects had a weak dependency on sample size, therefore, length scale changes did not affect the ignition delay time, surface temperatures, nor the critical heat flux for ignition. It was determined that the ignition delay time is affected by the flow characteristics mainly by changing the fuel mass fraction. A minimum mass fraction of fuel was found necessary for ignition to occur and this value remains invariant with all parameters studied.

KEYWORDS: Ignition, Flammability, Micro-gravity

INTRODUCTION

The possibility of an accidental fire occurring in a space-based facility during a long mission is a primary safety concern. For this reason, it is critical to characterize the fire properties of materials used in such facilities. The flammability requirements for all materials to be used in space vehicles (NASA specifications) are given in reference [1]. This document specifies two tests to be performed before a material is qualified for use in a space vehicle, the "Upward Flame Propagation Test" (Test 1) and the "Heat and Visible Smoke Release Rates

[+] Present Address: Exponent Failure Analysis Associates, 21 Strathmore Road Natick, MA01760, USA.
[*] Corresponding Author

Test" (Test 2). These two tests are expected to properly assess the flammability of a material in micro-gravity conditions. A list of the materials tested is provided in reference [2]. A general overview of fire safety practices is provided by Friedman [3] but the only existing work, to the knowledge of the authors, that addresses the relevance of these tests to material flammability for micro-gravity applications is that of Ohlemiller and Villa [4]. Ohlemiller and Villa, following the protocol of Test 1, studied pre-heating by external radiation and compared the results with tests conducted with the Cone Calorimeter (ASTM-E-1354) and the L.I.F.T. (ASTM-E-1321). A detailed review of this work and other relevant studies can be found in the review of Torero et al. [5].

The LIFT procedure consists of a piloted ignition test and a flame spread test that combined produce a "flammability diagram" [6,7]. This work will focus on aspects related to the piloted ignition test. A number of studies followed the original development of Quintiere [6]. Janssens [8] suggested an alternative method for calculating thermophysical property data such as ($k\rho c$) and (k) by incorporating the actual emisivity of the material, instead of $\varepsilon = 1$ [8]. Kashiwagi [9] and Atreya et al.[10], studied the effects of sample orientation and found that the surface temperature prior to ignition for vertical samples was higher than for horizontal samples. Simms [11] investigated the effects of pilot location and found that for each location there was a corresponding surface temperature prior to ignition. All these studies have provided a solid theoretical basis around piloted ignition and experimental validation to the use of the LIFT.

Fire literature has devoted attention to determine minimum length scales that guarantee that bench scale tests provide information that can be extrapolated to realistic scenarios. The main issue of concern has been the effect of scale increase, scale reduction has deserved very little attention. Space based environments are characterized by low airflow velocities, of the order of 0.1 m/s, thus flames in micro-gravity are expected to be laminar. Furthermore, safety constraints and material cost require the use of small samples. Therefore, for this particular application, it is of great importance to understand the effect of scale reduction. In this work the effect of scale reduction on piloted ignition of PMMA is addressed by using the LIFT.

BACKGROUND

Ignition of a solid fuel can be described as follows. The solid fuel sample is considered initially at ambient temperature, T_∞. After suddenly imposing an incident heat flux ($\dot{q}''_i$), the temperature of the solid fuel sample rises until the surface reaches the temperature at which the fuel first produces volatiles, this will be referred as the pyrolysis temperature (T_p). The time required for the fuel surface to attain T_p will be referred the pyrolysis time, t_p. After attaining T_p, increasing amounts of vapor (pyrolysate) leave the surface, mixe with the ambient oxidizer, and create a flammable mixture. This period will be referred as the flammable mixture time (t_m). A small temperature increase at the surface characterizes this period [9]. Fuel properties, flow and geometry determine the flammable mixture time and a characteristic surface temperature, T_m. If the mixture temperature is increased the reaction becomes self-sustained, at which point ignition occurs. This period corresponds to the induction time (t_i) and can be characterized by a gas phase ignition temperature (T_{ig}). Extending the analysis of Fernandez-Pello [12], the ignition time (t_{ig}) can be given by

$$t_{ig} = t_p + t_m + t_i \qquad (1)$$

In general, t_i and t_m can be considered small when compared to t_p and the fuel and oxidizer mixture can be considered to become flammable immediately after pyrolysis starts. Pyrolysis temperatures and times are thus referred as ignition temperature (T_{ig}) and ignition delay time (t_{ig}) [6,7] and equation (1) simplifies to $t_{ig} = t_p$ and T_{ig} can be defined as T_p. When addressing issues of scale, t_p and t_m will be affected by the changing nature of the convective flow, therefore, t_m can not be ignored. In contrast, the strong pilot and ambient oxygen concentration ensures a minimal induction time (t_i) and equation (1) can be re-written as:

$$t_{ig} = t_p + t_m \tag{2}$$

PYROLYSIS TIME (t_p)

The energy balance at the surface of the sample under radiative heating given by equation (3).

$$\dot{q}_s''(0,t) = a\,\dot{q}_i'' - \varepsilon\sigma(T^4(0,t) - T_\infty^4) - h_c(T(0,t) - T_\infty) \tag{3}$$

Where ($\dot{q}_s''$) is the net heat flux at the surface of the sample, ($\dot{q}_i''$) the imposed external heat flux, (a) is the absorptivity, (ε) the emissivity, (σ) is the Stefan-Boltzmann constant, (T(0,t)) is the surface temperature at time (t) and (h_c) the convective heat transfer coefficient. The classical analysis of the ignition process [6] assumes a linear approximation for the surface re-radiation. The radiative term is then defined as:

$$\varepsilon\sigma(T^4(0,t) - T_\infty^4) = h_r(T(0,t) - T_\infty) \tag{4}$$

Substituting (4) into (3) and assuming that the total heat transfer coefficient (h_T) is equal to the sum of the convective heat transfer coefficient (h_c) and the radiative heat transfer coefficient (h_r), expression (5) defines the net heat flux ($\dot{q}_s''$) at the surface of the solid.

$$\dot{q}_s''(0,t) = a\,\dot{q}_i'' - h_T(T(0,t) - T_\infty) \tag{5}$$

The differential formulation of the governing energy equation is given by:

$$\frac{\partial^2 T}{\partial y^2} = \frac{1}{\alpha}\frac{\partial T}{\partial t} \qquad \begin{array}{l} \text{B.C.} \\ y = 0, \; -k\dfrac{\partial T}{\partial x} = \dot{q}_s''(0,t) \\ t = 0 \qquad T = T_\infty \\ x \to \infty \end{array} \tag{6}$$

by taking the Laplace transformation, a general solution for the temperature at the surface temperature (T_s), can be obtained:

$$T_s = T_\infty + \overline{T}\left[1 - e^{t/t_c}\,\mathrm{erfc}\left((t/t_c)^{1/2}\right)\right] \tag{7}$$

Where $\overline{T} = \frac{a\,\dot{q}_i''}{(h_T)}$ can be defined as a characteristic temperature and, $t_c = \frac{k\rho c}{(h_T)^2}$ is defined as a characteristic time. To obtain the pyrolysis time (t_p) the surface temperature (T_s) is substituted by T_p and equation (7) can be rewritten as:

$$T_p = T_\infty + \overline{T}\left[1 - e^{t_p/t_c}\,\mathrm{erfc}\left((t_p/t_c)^{1/2}\right)\right] \tag{8}$$

The fuel sample is considered inert until attainment of T_p. Simplified solutions have been proposed in the literature [6, 10, 18]. To solve for the pyrolysis time (t_p) a first order Taylor series expansion of equation (8) is conducted. The range of validity of this expansion is limited, thus can not be used over a large range of incident heat fluxes. Consequently, the domain has to be divided at least in two. For this purpose a characteristic time to pyrolysis, $\bar{t}_p = \frac{k\rho c(T_p - T_\infty)^2}{[\dot{q}_s''(0,t)]^2}$ can be defined by scaling the boundary condition of equation (6). The first domain corresponds to high incident heat fluxes where the pyrolysis temperature (T_p) is attained very fast, $\bar{t}_p << t_c$. Application of the first order Taylor Series Expansion to equation (8) around $t_p/t_c \to 0$ yields the following formulation for the pyrolysis time (t_p):

$$\frac{1}{\sqrt{t_p}} = \frac{2}{\sqrt{\pi}}\frac{a}{\sqrt{k\rho c}}\frac{\dot{q}_i''}{(T_p - T_\infty)} \tag{9}$$

As can be seen from equation (9), the short time solution for the pyrolysis time (t_p) is independent of the total heat transfer coefficient term (h_T). For low incident heat fluxes $\bar{t}_p >> t_c$ the Taylor series expansion around $t_p/t_c \to \infty$ yields:

$$\frac{1}{\sqrt{t_p}} = \frac{\sqrt{\pi}\sqrt{k\rho c}}{h_T}\left[1 - \frac{h_T(T_p - T_\infty)}{a\dot{q}_i''}\right] \tag{10}$$

The use of the appropriate simplified solution will allow the evaluation of the pyrolysis time (t_p) over the entire domain of imposed incident heat fluxes. By making $t_p \to \infty$ in equation (10) a minimum external heat flux that will lead to attainment of the pyrolysis temperature (at thermal equilibrium) can be extracted

$$\dot{q}_{0,P}'' = \frac{h_T(T_p - T_\infty)}{a} \tag{11}$$

It is important to note that determination of the fuel material properties (a, k, ρ, c) by experimentally obtaining t_p in the domain where $t_p/t_c \to 0$ (high heat fluxes) will lead to values that are independent of the environmental conditions. In contrast, $\dot{q}_{0,P}''$ is dependent on h_T, therefore is affected by nature of the convective flow parallel to the surface and the adequate determination of re-radiation heat losses (h_r).

The Total Heat Transfer Coefficient (h_T)

Values for the total heat transfer coefficient (h_T) have been shown to vary with orientation and environmental effects. Examples of typical values found in the literature are: 8.0 Wm^2K^{-1} for natural turbulent convection and a vertical sample [7], 13.5 Wm^2K^{-1} for a horizontal orientation [10] and up to 15.0 W/m^2K^{-1} obtained by Mikkola and Wichman [13] while conducting experiments on a vertical orientation with wood. Equation (4) shows that the re-radiation term is independent of the sample length scale and orientation. In contrast, the convective term is dependent on length scale through the value of the convective heat transfer coefficient (h_c).

The Convective Heat Transfer Coefficient (h_c) and Mass Transfer Coefficient (h_m) The flow field created by the temperature gradient between the fuel and the flow surrounding it defines the convective heat transfer coefficient (h_c). The average Nusselt number for a vertical hot wall subjected to natural convective transport is given by Bejan [14]:

$$Nu \approx Ra_L^{1/4} \tag{12}$$

Where the Nusselt number (Nu) is given by: $Nu = \frac{h_c L}{k}$ and the Rayleigh number (Ra_L) by: $Ra_L = \frac{(V_B L)^2}{(\alpha \nu)}$. The characteristic velocity induced by buoyancy is: $V_B = \sqrt{\beta g_o L \Delta T}$, where $\Delta T = T_S - T_\infty$, ($g_o$) is the acceleration of gravity and the thermal expansion coefficient for the gas (β) is defined as $\beta = 1/T_\infty$, (α) is the thermal diffusivity, (ν) is the kinematic viscosity, and (L) is the characteristic length scale. The value of the average convective heat transfer coefficient, (h_c) is thus given by:

$$h_c = \left(\frac{k}{L^{1/4}}\right)\left(\frac{\beta g_o \Delta T}{\alpha \nu}\right)^{1/4} \tag{13}$$

The average convective heat transfer coefficient has a weak dependency on the length scale ($L^{-1/4}$). A reduction of the sample size from the nominal 155 mm to 50 mm will imply a 15% increase in the value of (h_c), and approximately 4% increase in the overall heat losses at the surface. The convective heat transfer coefficient is also a function of the temperature difference between the sample surface and the flow stream. Again, the dependency on the temperature difference is a weak one ($\Delta T^{1/4}$).

Once the sample has attained the pyrolysis temperature, T_p, the fuel vapor (pyrolysate) is diffused and convected outwards. Diffusion of fuel into the natural boundary layer is governed by the convective mass transfer coefficient (h_m) which is determined by the flow and geometrical characteristics. Mass transfer is generally characterized by the average Sherwood (Sh) number given by Bejan [14]:

$$Sh = \frac{h_m L}{D} \approx Le^{\frac{1}{3}} Ra_L^{\frac{1}{4}} \tag{14}$$

where (D) is the diffusion coefficient and ($Le = \frac{\alpha}{\nu}$) is the Lewis number. This gives the following dependency of the (h_m) on the characteristic length scale, (L):

$$h_m = \left(\frac{D^{2/3} \alpha^{1/12}}{L^{1/4}} \right) \left(\frac{\beta g_o \Delta T}{\nu} \right)^{1/4} \tag{15}$$

h_m has the same dependency on the length scale and temperature difference as the convective heat transfer coefficient (h_c), ($L^{-1/4}$, $\Delta T^{1/4}$). It needs to be noted a decrease in length scale results in an increase of both h_c and h_m. An increase in h_c results an increase in the pyrolysis time (t_P). In opposition, an increase in h_m will result in a decrease in the mixing time (t_m).

FLAMMABLE MIXTURE TIME (t_m)

Once the pyrolysis temperature (T_p) has been attained gaseous fuel begins to enter the boundary layer formed close to the surface of the material. In the presence of pyrolysis the energy balance at the surface (equation (5)) changes to:

$$\dot{m}_F''(t) L_v = a\dot{q}_i'' - h_T (T_p - T_\infty) - \dot{q}_s''(t) \tag{16}$$

Where (L_v) is the heat of gasification, $\dot{m}_F''(t)$ is an average mass flow rate that does not take into account the structure of the boundary layer, thus is independent of length scale. This approximation is only justified by the opposing effects of h_c and h_m on t_m. Rearranging and solving for the mass flow rate ($\dot{m}_F'(t)$) of fuel evolved after the pyrolysis time (t_P),

$$\dot{m}_F'(t) = \dot{m}_F''(t) L = \frac{a\dot{q}_i'' - h_T (T_p - T_\infty) - \dot{q}_s''(t)}{L_v} L \tag{17}$$

where "L" is the length of the sample. For $t<t_P$, $\dot{m}_F'(t) = 0$. The mass flow rate of fuel increases with time, instead the boundary layer can be considered steady-state. Ignition will occur when the concentration of fuel evolved at the surface has reached a minimum value at the pilot location ($Y_{F,ig}$) or a 'flammable' mixture. The average fuel concentration (Y_F) is:

$$Y_F = \frac{\dot{m}_F'}{\dot{m}_F' + \dot{m}_0'} \tag{18}$$

The characteristic time required for the fuel to migrate from the sample surface to the pilot location is neglected (characteristic natural convection velocity is of the order of 0.5 m/s).

Heat Conduction into the Sample ($\dot{q}_s''(t)$) An approximate solution for the time evolution of the heat conducted into the sample can be obtained by determining the temperature gradient at the surface ($\dot{q}_S''(t) = -k \left. \frac{\partial T(y,t)}{\partial y} \right|_{y=0^-}$) before pyrolysis starts ($t < t_p$) by means of equation (7). For $t > t_p$ the solution provided by equation (7) is no longer valid, therefore the one-dimensional heat conduction equation for a semi-infinite slab with a constant temperature

boundary condition needs to be solved. At the pyrolysis time (t_p), matching of the first derivative of the temperature distribution resulting from both solutions is necessary to guarantee a continuos distribution of $\dot{q}''_s(t)$. This requires the incorporation of a time shift (τ) in the constant temperature solution to match both expressions for $\dot{q}''_s(t)$ at t_p. From equation (7) the following expression is obtained for the net surface heat flux ($\dot{q}''_s(t)$) prior to the pyrolysis time (t_p):

$$\dot{q}''_s = \frac{k\overline{T}}{\sqrt{\alpha t_c}}\left[e^{\frac{t}{t_c}}\operatorname{erfc}\left(\left(\frac{t}{t_c}\right)^{\frac{1}{2}}\right)\right] \tag{19}$$

Now, at t_p, the surface heat flux ($\dot{q}''_s$) is given by:

$$\dot{q}''_c = \frac{k\overline{T}}{\sqrt{\alpha t_c}}\left[e^{\frac{t_p}{t_c}}\operatorname{erfc}\left(\left(\frac{t_p}{t_c}\right)^{\frac{1}{2}}\right)\right] \tag{20}$$

After T_p is attained, it is assumed that the surface temperature T_s will remain at T_p and the solution to the energy equation is given by:

$$\dot{q}''_s(t) = \left[\frac{k(T_p - T_0)}{\sqrt{\pi\alpha(t - t_p + \tau)}}\right] \tag{21}$$

where the time shift (τ) is given by: $\tau = \frac{1}{\alpha\pi}\left[\frac{k(T_p - T_0)}{\dot{q}''_c}\right]^2$

Mass Flow Rate of Oxidizer ($\dot{m}'_o$) To evaluate ($\dot{m}'_o$), the mass of oxidizer entrained in the boundary layer at the pilot, an integral approach of simultaneously solving the energy and momentum equations was applied [14]. Integration of the energy and momentum equations results in the following expressions for the conservation of energy (22) and momentum (23):

$$\frac{d}{dx}\int_0^\delta u(T_\infty - T)dy = \alpha\frac{\partial T}{\partial y}\bigg|_{y=0} \tag{22}$$

$$\frac{d}{dx}\int_0^\delta u^2 dy = -\nu\frac{\partial u}{\partial y}_{y=0}\bigg| + +g\beta\int_0^\delta (T - T_\infty)dy \tag{23}$$

It is assumed that Pr ≈1 therefore $\delta \approx \delta_T$ where (δ) is the momentum boundary layer thickness and (δ_T) is the thermal boundary layer thickness. Assuming Squire type profiles for u(x,y) and T(x,y) the mass flow of oxidizer ($\dot{m}'_o(x)$) can then be evaluated and is given by:

$$\dot{m}_o''(x) = \frac{\rho}{12}\left[g\beta(T_p - T_\infty)\frac{(80)^3 \alpha^2}{\frac{20}{21} + Pr} \right]^{\frac{1}{4}} x^{\frac{3}{4}} \qquad (24)$$

EXPERIMENTAL RESULTS

Experimental Apparatus

The LIFT apparatus consists of a radiant panel that imposes a radiant flux on the sample from approximately 10 – 65 kW/m^2. Ignition samples are nominally 155 mm x 155 mm, with a thickness that ensures the material will react as thermally thick. The sample is placed in front of the radiant panel that forms an angle of 15° with the sample surface. The heat flux distribution over the sample is nearly uniform where the sample and radiant panel are closest. An acetylene/air pilot is located directly above the specimen (Figure 1(a)). Tests were conducted with 12.7-mm thick samples of polymethylmethacrylate (PMMA) conditioned at 23±3°C and 50±5%R.H. for 24 hours. For each experiment, observations were recorded along with the ignition delay time, t_{ig}, and surface temperatures, T_S, using 32 gauge type K thermocouples. Contact of the thermocouple junction with the exposed surface of the sample became increasingly difficult as the imposed heat flux was decreased and after long periods of exposure [15]. The thermocouple junctions were found to either lose contact with the surface of the material or to sink into the sample. The former will result in noise in the temperature profile and the latter will only weakly reflect the temperature rise of the surface. The scattering of the data forced the use of twenty thermocouples, distributed evenly throughout the sample surface, to provide an adequate level of confidence.

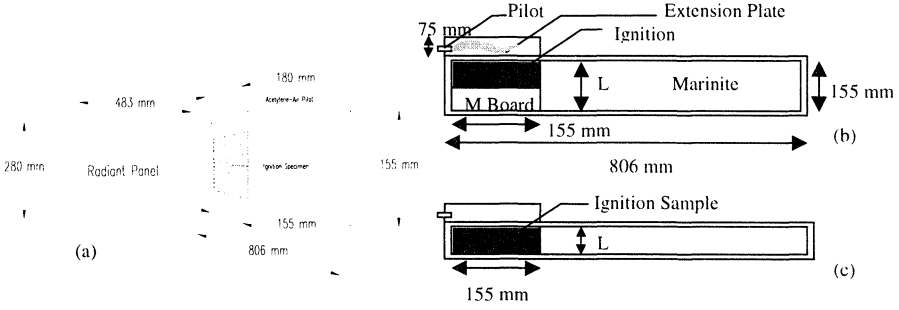

FIGURE 1 – Schematic of the experimental setup

The variation of the characteristic length scale of experiments was approached in two ways. One consisted of changing the fuel size and preserving the characteristic length scale (Figure 1(b)), while the second consisted of changing the characteristic length scale and consequently the magnitude of the flow that will bring the pyrolyzate to the pilot flame (Figure 1(c)). PMMA samples were scaled by decreasing the vertical length by 10 mm decrements to a final size of 25mm x 155mm. All tests were repeated at least eight times for varying levels of

incident heat flux from 9 to 50 kW/m^2. For the purpose of this analysis, experiments that failed to ignite in less than 1,200 seconds were considered to be non-ignitions.

The Surface Temperature

Surface temperatures, T_s, prior to ignition were measured for varying levels of imposed heat flux. Characteristic temperature histories are presented in Figure 2, the sample was exposed to radiation at t=0 and the peaks correspond to ignition (t_{ig},T_{ig}). The temperature increases faster for higher heat fluxes but no significant differences in T_{ig} were observed. From Figure 2 is impossible to define when pyrolysis starts, t_P and T_P, as opposed to ignition, t_{ig} and T_{ig}.

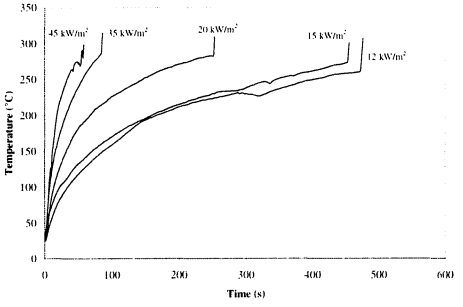

FIGURE 2 - Characteristic surface temperature histories for different incident heat fluxes.

Individual surface temperature histories do not provide an adequate estimation of the characteristic temperatures, since the scattering of the data can be of the order of 40°C. The thermocouple location seemed to have no systematic influence on the temperature measurements, except very close to the bottom of the sample. An average value obtained from all thermocouples, except those at the bottom edge, were used to extract a characteristic value for T_{ig}. For $\dot{q}''_i < \dot{q}''_{0,ig}$ the surface will attain thermal equilibrium at $T_{EQ}<T_{ig}$. Average values for T_{ig} and T_{EQ} are given in Figure 3. No ignition occurred for $\dot{q}''_i = \dot{q}''_{0,ig} < 11\,kW/m^2$. Figure 3 shows that no appreciable difference in T_{ig} can be noted for the range of heat fluxes tested 11-45 (kW/m^2). Surface temperatures prior to the onset of ignition were found to range between 250 °C and 288 °C. The mean value of a straight line fit through the data was used to determine an average surface temperature of the PMMA samples prior to ignition of T_{ig} = 273 °C. There is some discrepancy on the characteristic ignition temperatures reported in the literature. Quintiere and Harkleroad [7], reported a value of 378°C for type g PMMA (12.7mm thick) using the LIFT. Kashiwagi [9], reported surface temperatures of PMMA in a horizontal configuration to range between 360°C and 400°C, while Deepak and Drysdale [16] reported a lower value of 270°C for horizontal samples of PMMA. Thomson and Drysdale [15] reported a value of 310°C for PMMA samples in a horizontal configuration.

As mentioned before, Figure 2 does not allow for the determination of a characteristic temperature for the onset of pyrolysis (T_P). For this work T_P will be defined as the maximum possible T_{EQ} . This value is obtained by means of a line fit through the equilibrium temperature data and its intercept with the critical heat flux for ignition. For this particular case the value obtained is 263°C (Figure 3). It needs to be noted that although the value of T_p

does not represent the exact temperature of the onset of pyrolysis, its physical interpretation corresponds well with the assumption that the material is inert before a minimum temperature is attained.

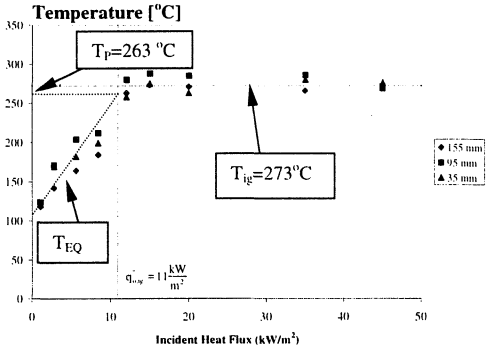

FIGURE 3 – Average ignition temperatures, T_{ig}, for different external heat fluxes, $\dot{q}_i''$. Data is presented for 3 different sample sizes but is characteristic of all sizes studied.

Minimum Fuel Mass Fraction for Ignition ($Y_{F,ig}$)

The time dependent average mass fraction of fuel at the pilot can be determined by means of equation (18). By finding the intercept between the ignition delay time and average mass fraction of fuel, the minimum average fuel mass fraction for ignition, ($Y_{F,ig}$), can be obtained. The value of $Y_{F,ig}$ is very consistent among tests. Figure 4 shows $Y_{F,ig}$ as a function of the external heat flux. In some cases where ignition did not occur after 1200 sec. it could be observed that the maximum value of Y_F had not yet reached the characteristic values determined for the cases where ignition was achieved. It can therefore be presumed that if the test was conducted for a longer period of time ignition might have been attained. As can be determined from Figure 4 the fuel mass fraction necessary for ignition varies in a range between 0.12 and 0.17 with values being almost unaffected by the sample size.

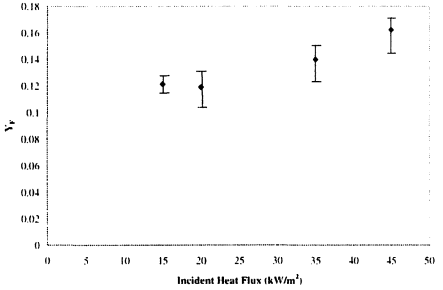

FIGURE 4 - Minimum fuel concentration for ignition ($Y_{F,ig}$) for different incident heat fluxes

Figure 4 shows that higher levels of incident heat flux reveal an increase in $Y_{F,ig}$. The steep slope of the mass fraction plots ($\partial Y_F/\partial t$), for the higher heat fluxes, could result in scattering

when determining fuel mass fraction, but the error bars presented in Figure 4 do not show such a trend. Instead the short ignition delay time maximizes the importance of other effects such as induction time, transport of fuel or other errors inherent to the protocol followed. Over estimation of the ignition delay time will result in an increase in $Y_{F,ig}$. The consistency of the values for the minimum fuel concentration necessary for ignition reveal another parameter that may be a tool in evaluating the flammability of solid materials.

Ignition Delay Time

The ignition delay time (t_{ig}) is presented in Figure 5, the choice of the $t_{ig}^{-0.5}$ vertical coordinate was made based on equation (9). Ignition did not occur at incident heat fluxes below 11 kW/m^2, therefore 11 kW/m^2 was deemed to be $\dot{q}''_{o,ig}$. Data is presented for different sample sizes and both geometrical configurations (Figure 1), only a few data points are presented but the results are characteristic of all experimental conditions studied. The data obtained was also compared with the results presented by Quintiere and Harkleroad [7] with very good agreement. It can be observed that all data collapses into one single curve, showing that the sample size and configuration have no significant effect on these parameters.

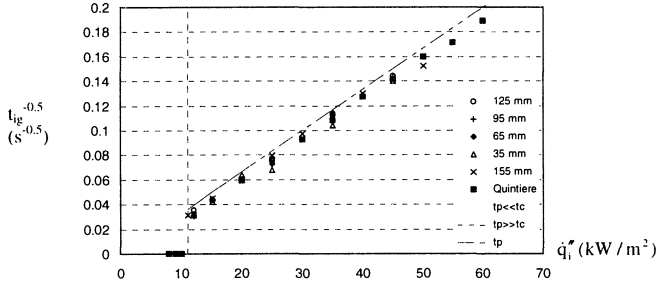

FIGURE 5 – Ignition delay time ($1/t_{ig}^{-0.5}$) for different external heat fluxes.

Together with the experimental data the predictions from equation (9) is presented. The value for $a/\sqrt{k\rho C}$ is extracted from the slope under the assumption that those properties do not vary between the onset of pyrolysis and ignition. By using the $Y_{F,ig}$ obtained in the previous section the ignition delay time is obtained (equation (2)). Both approximations are plotted (equations (9) and (10)), both showing a remarkable agreement with the experimental results.

CONCLUSIONS

For this specific material it was found that scaling has no significant effect on the time to attain the pyrolysis temperature or on the ignition delay time. Scaling analysis supported this conclusion by showing the weak dependency of heat and mass transfer on the characteristic length scale ($L^{-0.25}$). Natural convection has a significant influence on the heat balance at the surface, as shown by $\dot{q}''_{o,ig}$, but this effect is weakly affected by scale. T_{ig} was found to be invariant with the sample size and external heat flux. A minimum value for the fuel mass

fraction, $Y_{F,ig}$, at the pilot was found to be consistent for all length scales and heat fluxes. The experimental results presented show that, at least in what concerns the lateral ignition test, the LIFT apparatus can be scaled to meet the size criteria corresponding to safety needs of micro-gravity facilities. These results, although general in many aspects, should not be extrapolated to materials other than PMMA.

ACKNOWLEDGEMENTS

This work was funded by NASA Glenn under grant NAG-31961. The authors wish to thank Dr. Howard Ross from NASA Glenn and the help at UMCP of Alvaro Sifuentes.

REFERENCES

1. "Flammability, Odor, Offgassing, and Compatibility Requirements and test Procedures for Materials in Environments that Support Combustion," NASA-NHB 8060.1,1981.
2. "Materials Selection List for Space Hardware Systems," MSFC-HDBK-527-REV F, September 30, 1988.
3. Friedman, R., "Fire Safety in Spacecraft," Fire and Materials, 20, 235-243, 1996.
4. Ohlemiller, T.J. and Villa, K.M. "Material Flammability Test Assessment for Space Station Freedom," *NISTIR-4591*, National Institute of Standards and Technology, 1991.
5. J. L. Torero, N.J. Bahr, E. J. Carman, "Assessment of Material Flammability for Micro-Gravity Environments" 48th International Astronautical Federation Congress, Turin, Italy, *IAF-97-J.2.02*, October 1997.
6. Quintiere, J.G., "A Simplified Theory for Generalizing Results from a Radiant Panel rate of Flame Spread Apparattus," Fire and Materials, Vol.5, No.2, 1981.
7. Quintiere, J. G. and Harkleroad, M., "New Concepts for Measuring Flame spread properties," NBSIR-84-2943, National Bureau of Standards, 1984.
8. Janssens, M. L., "Thermal Model for Piloted Ignition of Wood Including Variable Thermophysical Properties," Fire Safety Science-3rd International Symposium, 167-176, 1991.
9. Kashiwagi, T., "Effects of sample Orientation on Radiative Ignition," Combustion and Flame, 44, 223-245, 1982.
10. Atreya, A., Carpenter, C., and Harkleroad, M., "The Effect of Sample Orientation on Piloted Ignition and Flame Spread," Fire Safety Science – 1st International Symposium, p.97-109, 1985.
11. Simms, D. L., "Experiments on the Ignition of Cellulosic Materials by Thermal Radiation," Combustion and Flame, 5, 369-375, 1961.
12. Fernandez-Pello, A.C., "The Solid Phase," Chapter 2, Combustion Fundamentals of Fire, Academic Press Limited, 1995.
13. Mikkola, E., and Wichman, I.S., "On the Thermal Ignition of Combustible Materials," Fire and Materials, 14, 87-96, 1989.
14. Bejan, A., Convection Heat Transfer, John Wiley and Sons, 1984.
15. Thomson, H.E., and Drysdale, D.D., "Flammability of Plastics, 1: Ignition Temperatures," Unit of Fire Safety Engineering, University of Edinburgh, UK.
16. Deepak, D., and Drysdale, D.D., "Flammability of Solids: An Apparatus to Measure the Critical Mass Flux at the Firepoint," Department of Fire Safety Engineering, University of Edinburgh, The King's buildings, Edinburgh EH9 3JL(UK).